NJC

Accepted Manuscript

This article can be cited before page numbers have been issued, to do this please use: M. safir filho, S. fiorucci, A. R. Martin and R. benhida, *New J. Chem.*, 2017, DOI: 10.1039/C7NJ03142D.

ROYAL SOCIETY OF CHEMISTRY

rsc.li/njc

View Article Online
DOI: 10.1039/C7NJ03142D

Design, Synthesis and Photophysical Studies of Styryl-Based Push-Pull Fluorophores with Remarkable Solvatofluorochromism

Mauro Safir Filho[†,‡], Sebastien Fiorucci[†], Anthony R. Martin[†,*] and Rachid Benhida[†,*]

[†] Université Côte d'Azur, CNRS, Institut de Chimie de Nice UMR7272, 06108 Nice, France
[‡] CAPES Foundation, Ministry of Education of Brazil, Brasília DF 70040-020, Brazil

Corresponding Authors
* anmartin@unice.fr, benhida@unice.fr

Abstract Graphic

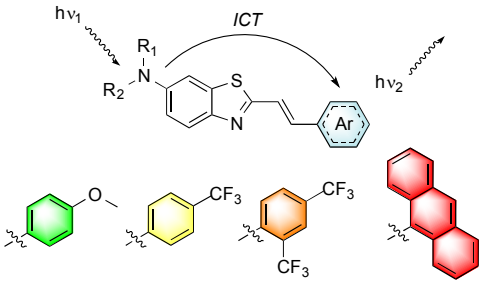

Abstract

A library of 20 styryl-based push-pull dyes derived from 6-amino substituted benzothiazoles were prepared by an efficient and practical synthetic route from low-cost starting materials. The dyes were firstly designed to present an effective anchoring site for subsequent conjugation. A series of aryl scaffolds, from substituted phenyl rings containing electron donating and withdrawing groups to polycyclic aromatic derivatives, were screened. The inductive effect of *N*-alkyl substituted benzothiazoles was also explored for three different arrangements. The investigation of the structure-photophysics relationship was performed by UV-vis absorption and steady-state fluorescence emission measurements in solution and by TD-DFT calculations. The dyes presented high brightness, absorption bands in the visible range (~ 370 - 453 nm) and large solvatofluorochromism comprising all the visible spectrum, as a consequence of the strong intramolecular charge transfer (ICT) nature of their excited state.

Introduction

The design and development of powerful fluorescent tools is a continuously expanding field of research.[1] Within this area, the quest for evermore bright, robust, fine-tuned and sensitive environment-responsive dyes has attracted a lot of attention.
Environment-sensitive dyes based on push-pull systems are a class of molecules that are able to change their spectroscopic properties in response to physical or chemical modifications in their microenvironment.[2] Push-pull solvatofluorochromic dyes, a known class of polarity-sensitive molecules, have the peculiar feature of displaying different emission maxima as a function of the polarity of the surrounding media (i.e. solvent). Thus, sensitive push-pull dyes have been the subject of intense research due to their wide range of potential applications including molecular probes,[3,4] fluorescent markers,[5–7] bioimaging,[8–10] ion sensing,[11,12] organic photovoltaics,[13,14] organic light-emitting diodes (OLED)[15] and photoresponsive materials[16–18] as a result of their linear and non-linear optical properties.[19] Structurally, these molecules feature an electron-donor moiety (D) and an electron-acceptor (A) group linked together through a π-conjugated system (D-π-A). This D-π-A arrangement may enable, upon photon irradiation, the formation of a photo-induced intramolecular charge transfer (ICT) excited state that generates dipole moments that enhance the fluorophore sensitivity to environment polarity.[20,21] Meanwhile, the range of the emission wavelength can be easily modulated by controlling the electronic properties of the donor and the acceptor groups.
In this context, styryl-based fluorophores constitute a common class of molecules exhibiting this D-π-A framework and encompass a broad variety of applications.[22] Nevertheless, while a range of diverse styryl-based dyes have been reported,[23–29] including derivatives of benzothiazoles,[30,31] studies focused on neutral, highly emissive and solvatofluorochromic styryl-benzothiazole scaffolds remain scarce in the literature.[6,32–34] In 2013, Herner et al.[6] described a class of fluorogenic dyes adaptable for direct bioconjugation via azido-alkyne cycloaddition albeit with relative reduced quantum yield. Ono and co-workers[32] reported two methylenemalononitrile-containing benzothiazole push-pull dyes with high affinity to probe αβ amyloid aggregates in the human brain. Finally, Bashmakova et al.[33] investigated the photophysical behavior of three new solvatofluorochromic styryl-benzothiazole dyes by steady state, time-resolved fluorescence techniques and computational calculations. There is still a need for a more comprehensive study devoted to the establishment of a robust structure-photophysics relationship in this peculiar class of dyes. This may prove helpful in the design of new fluorescent tools harboring optimized photophysical properties.
In line with the studies mentioned above that aim to access new fluorescent probes for practical applications, we report herein the synthesis of 20 styryl-based push-pull dyes derived from 6-aminobenzothiazoles. We decided to focus our work on these dyes where A is a σ-acceptor as no comprehensive structure-photophysics relationship were reported for this type of framework. Moreover, the presence of the 6-amino function can be beneficial for further modifications (Table 1). The study

View Article Online
DOI: 10.1039/C7NJ03142D

and analysis of this family of dyes has enabled us to understand the structure–photophysics relationship. It is noteworthy that heretofore only a small number of studies have been done to evaluate such relationships.[35–38] The synthesis of this family of highly solvatofluorochromic dyes, starting from simple and inexpensive 2-methylbenzothiazole, has allowed us to probe the influence of the three types of modifications of the central 2-styryl-6-aminobenzothiazole (Table 1): 1- the alkylation of the 6-amino function (D); 2- decoration of the phenyl ring of the styryl moiety with various electron-withdrawing (EWG) and electron-donating groups (EDG) (A); and 3- the replacement of this simple phenyl motif with larger frameworks (*e.g.* naphthyl, anthryl, etc.). Finally, we present the spectroscopic characterization and DFT calculations for dyes with distinct photophysical properties in terms of visible absorption and emission, brightness and Stokes shift. Altogether, we think that the detailed study presented herein could be used as a database for the design of fluorescent tools, based on the styryl-6-aminobenzothiazole motif, for specific applications.

Table 1. Chemical structure of the benzothiazole-based push-pull dyes.

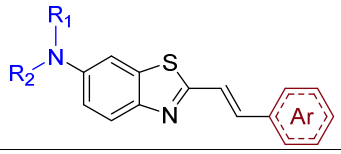

Dye	R_1	R_2	Ar
D1b	Ethyl	H	Phenyl
D2a	H	H	4-methoxyphenyl
D2b	Ethyl	H	4-methoxyphenyl
D2c	Ethyl	octyl	4-methoxyphenyl
D3b	Ethyl	H	4-(trifluoromethyl)phenyl
D4b	Ethyl	H	4-bromophenyl
D5b	Ethyl	H	2-(trifluoromethyl)phenyl
D6b	Ethyl	H	2,3-(dimethoxy)phenyl
D7b	Ethyl	H	3,4,5-(trimethoxy)phenyl
D8b	Ethyl	H	2,4-bis(trifluoromethyl)phenyl
D9b	Ethyl	H	*trans*-4-methoxy-β-styryl
D10b	Ethyl	H	4-biphenyl
D11a	H	H	1-naphthyl
D11b	Ethyl	H	1-naphthyl
D11c	Ethyl	octyl	1-naphthyl
D12b	Ethyl	H	2-methoxy-1-naphthyl
D13b	Ethyl	H	9-anthryl
D14a	H	H	1-pyrenyl
D14b	Ethyl	H	1-pyrenyl
D14c	Ethyl	octyl	1-pyrenyl

Results and Discussion

Synthesis of Benzothiazole Precursors 3 and 5. The precursor 6-amino-2-methylbenzo[d]thiazole (**3**) was synthesized starting from commercially available 2-methylbenzothiazole (**1**) in two steps in 57% overall yield (Scheme 1). Firstly, 2-methylbenzothiazole was converted to the respective 2-methyl-6-nitrobenzo[d]thiazole (**2**) by nitration at 0 °C using a stoichiometric amount of sodium nitrate in concentrated sulfuric acid as the nitrating mixture. The nitro derivative **2** was obtained in good yield (74%) as light yellow needles after recrystallization from ethanol.[39] Next, the treatment of a methanolic solution of **2** at room temperature with zinc powder and ammonium formate furnished the respective amino derivative **3** (77 %). Subsequent acylation of the amino group of **3** using 1.1 equivalents of acetyl chloride in dry DMF and in the presence of DIPEA afforded the *N*-acetamido derivative **4** in excellent yield (96 %). The synthesis of the key intermediate **5**, *N*-ethyl-2-methylbenzo[d]thiazol-6-amine, was accomplished by reduction of **4** using lithium aluminum hydride at room temperature for 12 hours. Compound **5** was obtained in high yield (87 %) after purification by flash column chromatography. This route was performed on a multigram scale to provide material for the subsequent steps.

Scheme 1.[a] Synthesis of benzothiazole precursors

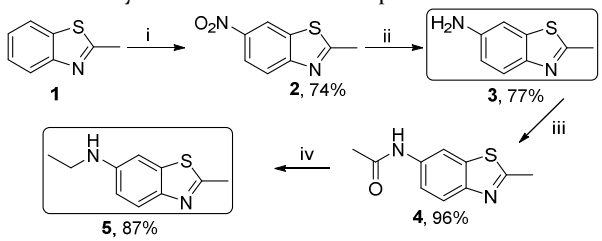

[a]Reagents and conditions: (i) $NaNO_3$, H_2SO_4, 0°C, 2 h, 74 %. (ii) Zn, NH_4COOH, methanol, r.t., overnight, 77 %. (iii) AcCl, DIEA, DMF, 0 - 20 °C, 1 h, 96 %. (iv) $LiAlH_4$, THF, r.t., 12 h, 87 %.

Dye synthesis. The synthetic route towards dyes **D1b-D14b** involves the aldol condensation between various aromatic aldehydes and the intermediate **5** that bears an activated methyl group on its 2-position (Scheme 2). The aromatic aldehydes

View Article Online
DOI: 10.1039/C7NJ03142D

were chosen to modulate the steric and electronic properties of the final dyes. For this family of compounds, either the parent benzaldehyde, or benzaldehydes that are mono/poly substituted with EWG (-CF_3, Br) or EDG (-OMe), were used. Cinnamaldehyde bearing *p*-OMe EDG was selected to investigate the influence of the length of the π-conjugated bridge. Bulkier aromatic aldehydes, such as 1-naphthaldehyde, were also employed. Importantly, we included polycyclic aromatic aldehydes able to promote excimer formation (9-anthryl and 1-pyrenyl radicals) in this study.

Scheme 2. Synthesis of dyes containing the *N*-ethyl-6-aminobenzothiazole core.

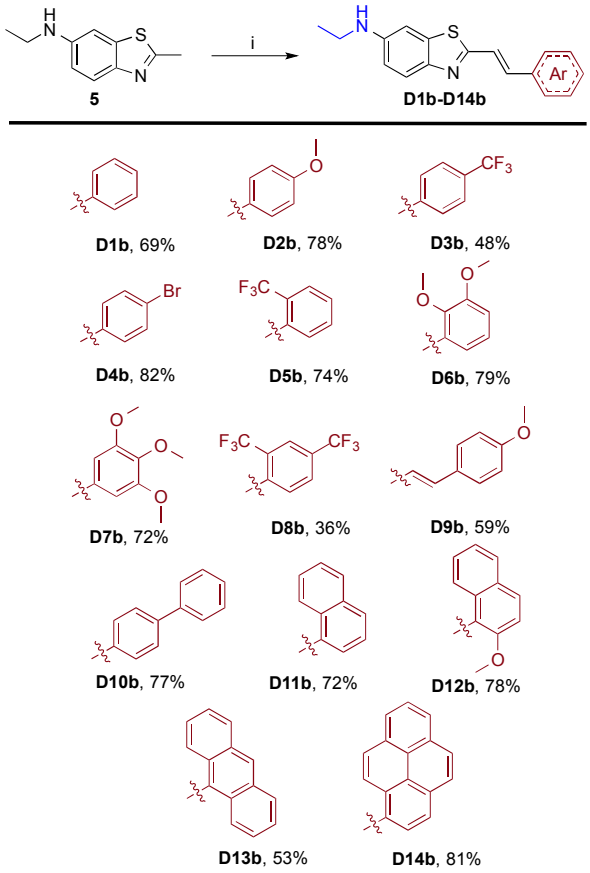

[a]Reagent and conditions: (i) aromatic aldehyde, KOH, DMF, r.t., sonication, 1 h.

The preparation of **D1b**-**D14b** was performed at room temperature with ultrasonic irradiation, in *N,N*-dimethylformamide using a stoichiometric amount of potassium hydroxide. It is worth mentioning that attempts to use milder bases such as tertiary amines or sodium acetate did not afford any product. On the contrary, potassium *tert*-butoxide behaved similarly to hydroxide and proved efficient in the activation of the 2-methyl group of **5**. Thus, using KOH as the base, all dyes (**D1b**-**D14b**) were isolated in satisfactory yield (36-82 %) after purification by chromatography. Finally, to ensure the high purity required for photophysical studies, **D1b**-**D14b** were further recrystallized from methanol (12-49 % yield).

Next, the completion of this family of dyes was pursued by synthesizing two more series in which the 6-amino function of precursor **3** either remains as a primary amine or is converted to the tertiary *N*-ethyl-*N*-octyl-6-amino derivative. These two series enable the evaluation of the inductive effect of the alkyl substituents on the donating ability of the amino group attached to the benzothiazole scaffold (Scheme 3). Dyes bearing the primary amino group (**D2a**, **D11a** and **D14a**) were accessed in a similar way to dyes **D1b**-**D14b** but starting from the benzothiazole precursor **3** instead of **5**. For the second series, the tertiary amino derivatives **D2c**, **D11c** and **D14c** were obtained in excellent yields (80-88 %) by alkylation of the corresponding dye (**D2b**, **D11b** and **D14b**) using 1-iodooctane in the presence of potassium carbonate (Scheme 3). Interestingly, no byproducts corresponding to the quaternarization of the endocyclic nitrogen in the thiazole ring was observed. Hence, this simple and straightforward transformation could also be employed in the design and preparation of valuable spectroscopic tools; for instance, this easy entry to dye modification could be used in the tailoring of membrane probes or for biolabeling experiments.

Scheme 3. Synthesis of dyes bearing a primary or tertiary 6-amino function.

View Article Online
DOI: 10.1039/C7NJ03142D

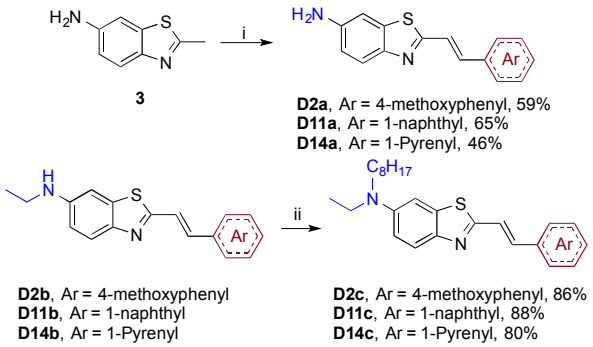

[a]Reagent and conditions: (i) aromatic aldehyde, KOH, DMF, r.t., sonication, 1 h. (ii) 1-iodooctane, K_2CO_3, acetonitrile, 80°C, 24 h.

Photophysical Studies

Substituted Phenyl Series: Dyes D1b-D9b.

The photophysical properties in various solvents for **D1b**-**D9b** are summarized in Table 2.

Table 2. Relevant photophysical data from UV-visible absorption and fluorescence emission of dyes **D1b**-**D9b**

Solvent $E_T(30)$[a]	Varied phenyl substituents (acceptor)/Fixed 6-ethylamino- (donor)									
	λ, $\Delta\lambda_{ST}$[b], Φ_{fl}[c]	**D1b**	**D2b**	**D3b**	**D4b**	**D5b**	**D6b**	**D7b**	**D8b**	**D9b**
ε × 10^3 ($M^{-1}.cm^{-1}$)		25.4	48.3	27.1	36.8	34.4	34.3	41.1	38.1	62.4
Cyclohexane (30.9)	λ_{abs}	380	380	394	389	389	379	384	407	401
	λ_{em}	445	447	463	456	462	449	450	487	473
	$\Delta\lambda_{ST}$	3843	3944	3782	3777	4062	4113	3819	4036	3796
	Φ_{fl}	0.81	0.58	0.63	0.56	0.78	0.53	0.50	0.80	0.44
Toluene (33.9)	λ_{abs}	385	386	400	394	394	386	390	414	409
	λ_{em}	467	464	484	471	483	468	470	516	491
	$\Delta\lambda_{ST}$	4560	4355	4338	4149	4677	4539	4364	4775	4083
	Φ_{fl}	0.83	0.75	0.67	0.66	0.64	0.65	0.83	0.83	0.57
1,4-Dioxane (36.0)	λ_{abs}	387	387	398	395	396	388	390	415	409
	λ_{em}	474	469	497	482	499	475	474	533	498
	$\Delta\lambda_{ST}$	4742	4517	5005	4569	5212	4720	4544	5334	4369
	Φ_{fl}	0.73	0.79	0.74	0.57	0.70	0.63	0.74	0.76	0.63
Ethyl acetate (38.1)	λ_{abs}	385	384	400	394	395	387	388	416	406
	λ_{em}	486	476	521	501	518	487	484	565	507
	$\Delta\lambda_{ST}$	5398	5033	5806	5420	6011	5306	5112	6339	4906
	Φ_{fl}	0.61	0.74	0.47	0.56	0.68	0.62	0.61	0.57	0.48
DMSO (45.1)	λ_{abs}	400	399	417	409	415	404	403	438	421
	λ_{em}	530	514	575	546	572	531	526	630	549
	$\Delta\lambda_{ST}$	6132	5607	6589	6134	6614	5920	5802	6958	5538
	Φ_{fl}	0.67	0.78	0.78	0.87	0.85	0.79	0.76	0.61	0.68
MeCN (45.6)	λ_{abs}	384	385	398	393	395	386	390	412	405
	λ_{em}	510	495	549	525	549	512	507	600	528
	$\Delta\lambda_{ST}$	6434	5772	6911	6397	7101	6375	5917	7605	5751
	Φ_{fl}	0.63	0.64	0.52	0.50	0.59	0.45	0.73	0.55	0.46
MeOH (55.4)	λ_{abs}	389	390	405	398	401	393	393	422	408
	λ_{em}	519	509	548	529	547	521	519	591	536
	$\Delta\lambda_{ST}$	6439	5994	6443	6222	6656	6251	6177	6776	5853
	Φ_{fl}	0.57	0.61	0.52	0.52	0.68	0.52	0.53	0.65	0.45

[a] Reichardt's $E_T(30)$ was selected to measure solvent polarity.[20] [b] Stokes shifts ($\Delta\lambda_{ST}$) are reported in cm^{-1}. [c] Fluorescence quantum yields (Φ_{fl}) were measured using quinine sulfate in an aqueous 0.1 M $HClO_4$ solution (λ_{exc} = 350 nm, Φ_{fl} = 0.59) or fluorescein in 0.1 M NaOH aq. solution (λ_{exc} = 475 nm, Φ_{fl} = 0.89) as the references.[40]

To evaluate the influence of the phenyl substituents on the spectroscopic behavior of the dyes, we varied these substituents while keeping the donor group (ethylamino-) on the benzothiazole scaffold unchanged. Dye **D1b**, containing an unsubstituted phenyl ring was chosen as the reference. All of the dyes **D2b**-**D8b** containing substituted phenyl rings absorbed more strongly than **D1b** (27.1 - 48.3 × 10^3 $M^{-1}.cm^{-1}$ *vs.* 25.4 × 10^3 $M^{-1}.cm^{-1}$, respectively), with **D2b** (*p*-OMe) presenting the highest hyperchromic

View Article Online
DOI: 10.1039/C7NJ03142D

effect of this series. Additionally, all dyes presented absorption bands in the visible range (384 - 412 nm in acetonitrile), with ε values in agreement with π-π^* electronic transitions. Large Stokes shifts in polar solvents, *ca.* 5751 - 7605 cm^{-1} in acetonitrile, were also observed. The relatively weak solvent dependence in the absorption maxima of **D1b**-**D9b** indicates that the stabilization energy for the ground S_0 and the Franck-Condon state of S_1 are quite similar. In contrast, they showed gradually increased bathochromic shifts in their emission maxima when going from the least polar aprotic solvent to the most polar solvent (Table 2, Figure 1). Using **D1b** as the reference, dyes containing *para*-substituted phenyl rings (**D2b**-**D4b**), presented similar absorption spectra, whereas the emission maxima was slightly blue-shifted for dye **D2b** that bears an EDG (*p*-OMe), and red-shifted for dyes containing EWGs (**D3b**, *p*-CF_3 and **D4b**, *p*-Br), in polar solvents. Fluorescence quantum yields for dyes **D1b**-**D9b** were in the 0.44 - 0.87 range for all the tested solvents; no strong dependence on the solvent polarity was observed. In this series, dye **D8b** that features the 2,4-*bis*(trifluoromethyl)phenyl pattern exhibited the most accentuated solvent sensitivity as indicated by the largest red-shift of its emission maxima (Figure 2). Additionally, the *ortho* or *para* positioning of the -CF_3 substituent (**D3b** and **D5b**) does not significantly affect either the absorption or emission maxima, while increasing the number of OMe groups (dye **D6b** and **D7b**), regardless of their location, resulted in a moderate bathochromic shift in the emission maxima in polar solvents, compared to **D2b**.

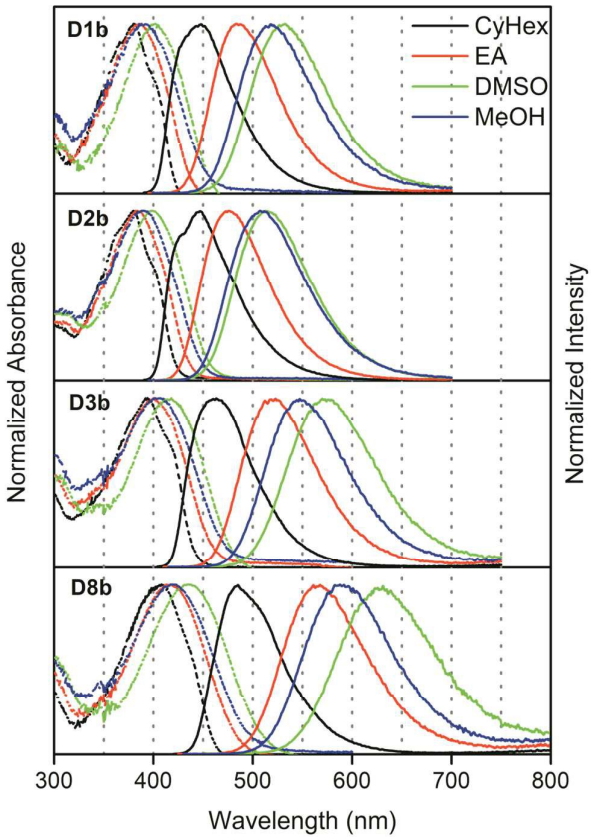

Figure 1. Absorption (dashed) and fluorescence emission (solid) spectra of dyes **D1b**, **D2b**, **D3b** and **D8b** in cyclohexane (black), ethyl acetate (red), DMSO (green) and MeOH (blue).

The influence of the alkene bridge length between the benzothiazole and the phenyl ring on the spectroscopic properties was evaluated by comparing dyes **D2b** and **D9b**; the latter bears an additional vinyl unit. The absorption maximum for **D9b** was equally red-shifted, by about 20 nm, in all the tested solvents. This effect was accompanied with an increase in the molar extinction coefficient ε (+29 %, compared to **D2b**), as a consequence of its higher degree of conjugation. Moreover, it is interesting to note that the λ_{abs} redshift, related to the additional vinyl unit, is significantly lower compared to similar cationic[41] and neutral[42,43] polymethine dyes. In contrast with the absorption maximum of **D9b**, the fluorescence emission spectra showed some degree of solvent dependency, especially for the most polar media. In fact, while the λ_{em} difference between **D9b** and **D2b** is only 26 nm in cyclohexane, it reached 35 nm in DMSO.

The sensitivity of the dyes to solvent polarity was evaluated by plotting the Stokes shifts *vs* Reichardt's $E_T(30)$ scale (Figure 2 and Figure S2). This latter quantitative parameter accounts for the dielectric constant of the solvent and its hydrogen-bond donor ability.[20] Among the first series of dyes (**D1b**-**D9b**), **D8b** showed the highest sensitivity (highest slope, Figure 3). As a general trend, more structured emission band were observed in cyclohexane. This may be due to some degree of contribution from a locally excited (LE) state emission.[44] However, the large positive solvatofluorochromism and the proportionally red-shifted emission maxima for the dyes along the range of polarity strongly suggest the formation of a relaxed ICT state in solvents of increasing polarity. Moreover, the fact that only a single and broad structureless emission band is observed for all the dyes also supports the hypothesis of a fluorescence emission from an ICT state. In addition, the relatively intense fluorescence emission, even in polar environments, hints that the geometry of the ICT excited state seems to be close to the ground state and contributions associated to the formation of a non-coplanar TICT state may not be extensively involved. Emissive CT states are known to be associated with molecular rigidity; however, the strength of the donor/acceptor groups are

View Article Online
DOI: 10.1039/C7NJ03142D

also important to modulate TICT formation.[45] Examples of highly emissive ICT excited states in highly polar solvents are known in the literature either in the case of rigid molecular scaffolds or non-rigid architectures including chalcone,[46] courmarin[45] and fluorene dyes.[38] Differences between the dipole moments (μ_e - μ_g) of the ground and excited states of the dyes was estimated by plotting the Stokes shifts as a function of the Lippert-Mataga orientation polarizability (Δf) parameter[47,48] (Supporting Information, Figure S2 and Table S1). Values of 10.3, 9.9, 11.7 and 13.4 D, for μ_e - μ_g, were obtained for dyes **D1b**, **D2b**, **D3b** and **D8b**, respectively. The increase in the excited state dipole moment is accomplished by a higher level of charge separation between the donor (6-ethylamino) and the acceptor (aryl group). Hence, since the donor group remained unchanged in this series, the largest charge separation, corresponding to the highest μ_e - μ_g difference, was observed for **D8b** that features the most electron-poor arene (2,4-*bis*-CF_3) on the acceptor moiety.

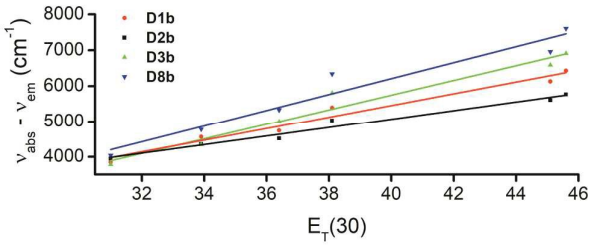

Figure 2. Dependence of the Stokes shift on the empirical polarity parameter E_T(30) for dyes **D1b**, **D2b**, **D3b** and **D8b**. Correlation factors R^2 are, respectively, 0.96, 0.97, 0.95and 0.93. The linear plots shown were obtained with all the tested solvents except methanol.

To complete the spectroscopic study, the dyes were further investigated by DFT calculations at the MPW1PW91/6-311+G(d,p) level of theory, using Gaussian 03. Optimized ground-state geometries were found to be close to planar for all dyes except for those presenting *ortho*-substituents (**D5b, D6b** and **D8b**), where the phenyl ring appeared slightly twisted respectively to the 2-vinylbenzothiazole motif (Figure S3). The calculations revealed that the less energetic electronic transitions occur between the frontier molecular orbitals HOMO and LUMO. The highest occupied molecular orbital (HOMO) is partially localized on the benzothiazole donor and around the vinyl bridge while the lowest unoccupied molecular orbital (LUMO) is spread across the bridge and the phenyl ring (Figure 3). Compared with other dyes, the LUMO of **D8b** features a higher electronic density on its acceptor motif (2,4-*bis*-(CF_3)). This strongly supports the large ICT character that was observed for this dye. Furthermore, for **D1b-D3b** and **D8b**, time-dependent (TD)-DFT calculations in cyclohexane and DMSO yielded their corresponding calculated absorption maxima associated to the first electronic transition $S_o \rightarrow S_1$. Compared with the experimental values, the calculated absorption maxima followed the same trend and were only slightly red-shifted (see Supporting Information).

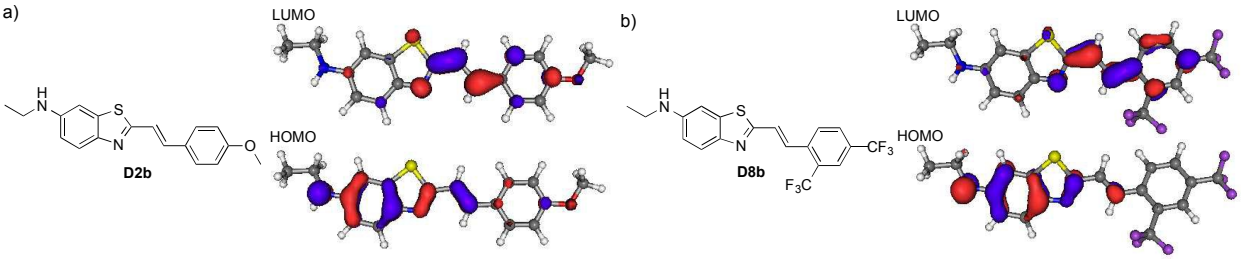

Figure 3. Representation of HOMO and LUMO, for dyes **D2b** (a) and **D8b**(b), obtained from optimized ground state geometries.

Finally, to overcome the challenges in predicting the emission maxima and Stokes shifts by DFT calculations, the correlation between λ_{em} and $\Delta\lambda_{ST}$ (in wavelength) for dyes containing *para*-substituted phenyl rings was performed using the σ_p Hammett substituent parameter model.[49] Dye **D1b** was selected as reference (σ_p = 0), while dyes **D2b**, **D3b** and **D4b** were selected as representative dyes containing EDG and EWG. Figure 4 depicts the plots of emission maxima and Stokes shift *vs* σ_p for five different solvents. Excellent correlations for the λ_{em} were achieved for all solvents (R^2= 0.94 - 0.98) except for those of low polarity (cyclohexane and toluene, see Supporting Information). In parallel, linear trend between Stokes shift and σ_p values was obtained exclusively for solvents with moderate and high polarity (1,4-dioxane to methanol), with R^2 values ranging from 0.80 to 0.98. To verify our prediction model, the emission maxima and the Stokes shift for the reported dye **D1b** were calculated for five solvents. The values were slightly shifted compared to the experimental ones (Table S2), with errors in an acceptable range (± 3 nm for both λ_{em} and $\Delta\lambda_{ST}$).

View Article Online
DOI: 10.1039/C7NJ03142D

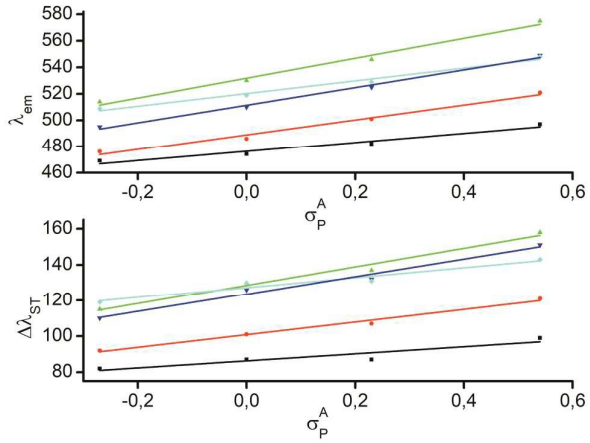

Figure 4. Dependence of the emission maxima (up) and Stokes shift (down) of **D1b**, **D2b**, **D3b** and **D4b** on the Hammett values (σ_p) in methanol (cyano), acetonitrile (blue), dimethyl sulfoxide (green), ethyl acetate (red) and 1,4-dioxane (black). Correlation factors R^2 are, respectively, 0.94, 0.98, 0.98, 0.99 and 0.98 related to λ_{em} and 0.80, 0.98, 0.97, 0.97 and 0.92 related to $\Delta\lambda_{ST}$.

Polycyclic Aromatic Hydrocarbon Series

To get further insight into the effect of the acceptor moiety on the photophysical properties of the dyes, different polycyclic aromatic hydrocarbons were evaluated using the same benzothiazole scaffold while keeping the 6-ethylamino function unchanged. The corresponding data are presented in Table 3. Figure 5 depicts the UV-visible and fluorescence emission spectra of dyes **D10b**-**D14b** in four representative solvents.

Table 3. Relevant photophysical data from UV-visible absorption and fluorescence emission of dyes **D10b**-**D14b**

Solvent	Varied polycyclic aromatic (acceptor)/Fixed 6-ethylamino- (donor)				
	λ, $\Delta\lambda_{ST}$, Φ_{fl}	**D10b**	**D11b**	**D12b**	**D13b**	**D14b**
$\varepsilon \times 10^3$ ($M^{-1}.cm^{-1}$)		44.7	37.3	36.8	28.9	54.6
Cyclohexane (30.9)	λ_{abs}	391	383	386	400	418
	λ_{em}	464	475	478	557	508
	$\Delta\lambda_{ST}$	4024	5057	4986	7047	4238
	Φ_{fl}	0.63	0.37	0.42	0.47	0.68
Toluene (33.9)	λ_{abs}	398	392	396	408	428
	λ_{em}	479	491	494	571	526
	$\Delta\lambda_{ST}$	4249	5143	5009	6996	4353
	Φ_{fl}	0.77	0.47	0.30	0.48	0.71
1,4-Dioxane (36.0)	λ_{abs}	399	395	397	407	427
	λ_{em}	487	502	503	581	531
	$\Delta\lambda_{ST}$	4529	5396	5308	7358	4586
	Φ_{fl}	0.60	0.45	0.48	0.40	0.73
Ethyl acetate (38.1)	λ_{abs}	396	393	394	405	425
	λ_{em}	507	519	513	600	558
	$\Delta\lambda_{ST}$	5528	6177	5887	8025	5608
	Φ_{fl}	0.48	0.51	0.47	0.36	0.60
DMSO (45.1)	λ_{abs}	413	412	414	419	443
	λ_{em}	557	571	559	674	621
	$\Delta\lambda_{ST}$	6259	6758	6265	9029	6470
	Φ_{fl}	0.79	0.82	0.75	0.36	0.65
MeCN (45.6)	λ_{abs}	396	393	396	404	425
	λ_{em}	531	548	537	639	591
	$\Delta\lambda_{ST}$	6420	7197	6630	9103	6608
	Φ_{fl}	0.52	0.54	0.43	0.33	0.59
MeOH (55.4)	λ_{abs}	401	399	402	412	429
	λ_{em}	533	548	536	628	580
	$\Delta\lambda_{ST}$	6176	6814	6218	9139	6068
	Φ_{fl}	0.55	0.70	0.48	0.31	0.63

View Article Online
DOI: 10.1039/C7NJ03142D

See Table 2.

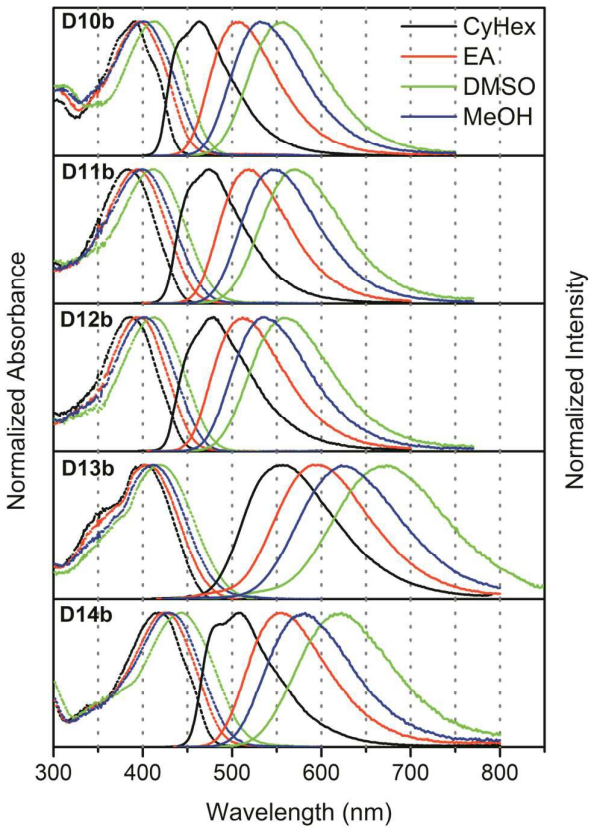

Figure 5. Absorption (dashed) and fluorescence emission (solid) spectra of dyes **D10b**-**D14b** in cyclohexane (black), ethyl acetate (red), DMSO (green) and MeOH (blue).

Similarly to the phenyl series (**D1b**-**D9b**), dye **D1b** was again selected as the reference. All dyes containing polycyclic aromatic groups, **D10b-D14b**, showed stronger absorption than **D1b** (28.9 - 54.6 × 10^3 $M^{-1}.cm^{-1}$ *vs.* 25.4× 10^3 $M^{-1}.cm^{-1}$, in dioxane). The absorption maxima for compounds containing up to three fused phenyl rings (**D11b-D13b**) exhibited a moderate bathochromic shift (9-20 nm in acetonitrile) compared with **D1b**. In contrast, replacing the phenyl ring with a bulky 1-pyrenyl core (**D14b**) strongly red-shifted the maximum (~ 40 nm in all the tested solvents) as a result of its higher degree of conjugation. Furthermore, this series, **D10b-D14b**, showed little dependency on the solvent polarity in their $\lambda_{abs,}$ thus supporting the hypothesis of a weak charge transfer character in their ground state. In contrast with their absorption maxima, the fluorescence emissions were affected in a similar manner to the phenyl derivatives **D1b-D9b**. Indeed, a high degree of solvent polarity dependency on λ_{em} was observed ($\Delta\lambda_{ST}$ up to 9103 cm^{-1} in acetonitrile).

Dye **D13b**, containing the 9-anthryl scaffold, showed the broadest absorption band with the lowest ε value among the polycyclic aromatic hydrocarbon derivatives. Additionally, the large shoulder around 350 nm may indicate a lack of planarity and that the resulted absorption band could contain a high contribution from a twisted anthracene moiety. This hypothesis was supported by the optimized DFT structure of **D13b** (Figure 6). It showed both a non-coplanar orientation of the 9-anthryl and vinylbenzothiazole motifs as well as a high electronic density located on the anthryl framework in the frontier orbitals. Compared with the other dyes of the same series, **D13b** presented distinct emission behavior with the lowest fluorescence quantum yield in polar solvents. It displayed an incredible mega-Stokes shift in DMSO (*ca.* 9029 cm^{-1} / 255 nm), in the same range that was observed for highly solvatochromic fluorene dyes with a methylenemalononitrile acceptor.[38] In addition, the intriguing highly red-shifted and broad structureless emission band observed in cyclohexane ($\Delta\lambda_{ST}$ = 7046 cm^{-1} / 157 nm) may suggests that a highly dipolar state is also formed in nonpolar environments. Based on photophysical studies concerning derivatives of 4-(9-anthryl)-*N*,*N*′-dimethylaniline (ADMA) and analogues,[50,51] we suspect that the strong electron acceptor character of the anthracene group in the excited state may favor an intramolecular electron transfer mechanism from the 6-*N*-ethylamino group to the anthryl radical, thus yielding an highly dipolar structure (D^{+}•A^{-}•) with reduced fluorescence emission.

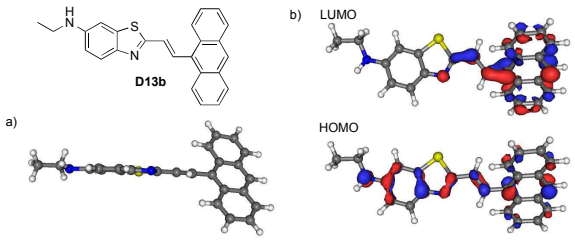

Figure 6. a) Optimized DFT structure of **D13b**. b) Frontier orbitals obtained from optimized ground state geometry.

View Article Online
DOI: 10.1039/C7NJ03142D

As for the first series, a linear correlation between the Stokes shifts of dyes **D10b**-**D12b** and **D14b** and the solvent polarity ($E_T(30)$ - Figure 7) was evidenced in this second series, except for **D13b** in which the reduced slope does not correlate with the photophysical data (see Supporting Information). This last observation may indicate that emission takes place from a distinct and highly polar CT state (*e.g.* involving an electron transfer process). The calculated values of μ_e - μ_g for dyes **D10b**-**D12b** and **D14b** (11.7, 10.6, 10.2 and 12.4 D, respectively, Figure S2, Table s2) are in agreement with the spectroscopic observation and support the strong charge transfer character for these dyes in the excited state. Finally, further investigations to highlight a putative excimer emission for the pyrene-containing dye, **D14b**, was performed. Surprisingly, no strong evidence associated with an excited state dimer emission was observed regardless of the broad range of concentrations or the different solvents that were probed (Figure S5). Nevertheless, these observations do not rule out the possibilities of designing dyes derived from **D14b** as fluorescent ratiometric monomer-excimer emitting probes.

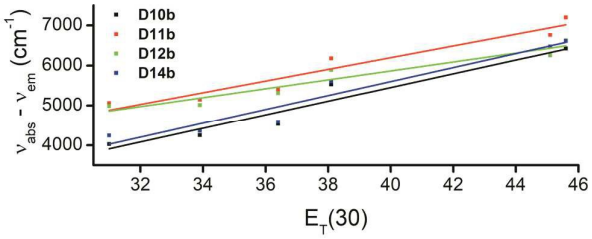

Figure 7. Dependence of the Stokes shift on the empirical polarity parameter $E_T(30)$ for dyes **D10b**-**D12b** and **D14b**. Correlation factors R^2 are, respectively, 0.93, 0.92 and 0.92. The linear plots shown were obtained with all the tested solvents except methanol.

Spectroscopic Impact of the Alkykation of the 6-Amino Functional Group

The last part of our study aimed to evaluate the effect of the alkyl radicals attached to the 6-amino group of the benzothiazole ring on the spectroscopic properties of the dyes. For this purpose, dyes **D2**, **D11** and **D14** bearing either a primary (**D2a**, **D11a** and **D14a**), a secondary (**D2b**, **D11b** and **D14b**) or a tertiary amine at the 6-position of the benzothiazole (**D2c**, **D11c** and **D14c**) were compared. Figure 8 depicts the UV-Vis absorption and fluorescence emission spectra for dyes **D2a-c**, **D11a-c**, and **D14a-c**, in cyclohexane and acetonitrile. Additional photophysical data are reported in the Table 4. As expected and in agreement with their positive inductive effect, increasing the number of alkyl substituents on the 6-amino group resulted in a gradual red-shift of both absorption and emission maxima (~ 10 to 15 nm per alkyl substituent). In addition, more structured emission bands in cyclohexane are also observed for dyes containing dialkyl substituted amines. It may be a consequence of the increased hydrophobicity and the loss of the hydrogen bond formation ability, thereby reducing the intermolecular dye-dye interactions. The main spectroscopic properties (ε, Φ_f, and Δλ) were moderately different among the dye families (**a**, **b** and **c**). Dyes **D2a** and **D11a**, bearing the primary amine, showed reduced fluorescence quantum yield and higher ε values, in comparison with their analogues **D2c** and **D11c**, respectively In contrast, dyes **D14a** and **D14c** presented similar Φ_f values, especially in polar solvents, with a higher extinction coefficient for **D14c**. Linear trends between the Stokes shift and the solvent polarity parameters $E_T(30)$ and *Δf* were also obtained (see Supporting Information).The transition dipole moments were directly correlated with the number of alkyl substituent on the amino group, with dyes bearing the tertiary amine presenting larger μ_e - μ_g values (Table S1, Supporting Information). Finally, the attachment of a second alkyl substituent on the 6-amino position (**D2c**, **D11c**and **D14c**) does not significantly reduce the brightness ($\varepsilon.\Phi_f$), when compared to the analogue containing the secondary *N*-ethylamine EDG (**D2b**, **D11b** and **D14b**).

Table 4. Relevant photophysical data from UV-visible absorption and fluorescence emission of dyes containing primary (**D2a**, **D11a** and **D14a**) and tertiary amines (**D2c**, **D11c** and **D14c**)

Solvent		Varied amine/Fixed aryl					
	λ, $\Delta\lambda_{ST}$, Φ_{fl}	**D2a**	**D2c**	**D11a**	**D11c**	**D14a**	**D14c**
$\varepsilon\times 10^3$ ($M^{-1}.cm^{-1}$)		37.7	33.1	34.4	29.7	54.2	65.9
Cyclohexane (30.9)	λ_{abs}	368	395	370	403	410	438
	λ_{em}	433	459	461	466	488	527
	$\Delta\lambda_{ST}$	4079	3529	5335	3354	3898	3855
	Φ_{fl}	0.25	0.69	0.37	0.49	0.73	0.65
Toluene (33.9)	λ_{abs}	374	401	378	413	417	443
	λ_{em}	449	480	480	497	508	547
	$\Delta\lambda_{ST}$	4466	4104	5621	4092	4295	4291
	Φ_{fl}	0.33	0.80	0.25	0.66	0.69	0.80
1,4-Dioxane (36.0)	λ_{abs}	379	400	380	413	417	441
	λ_{em}	463	480	492	514	517	545
	$\Delta\lambda_{ST}$	4786	4166	5990	4757	4638	4327
	Φ_{fl}	0.40	0.76	0.28	0.45	0.61	0.54
Ethyl acetate(38.1)	λ_{abs}	374	396	382	410	416	439
	λ_{em}	466	487	507	531	539	569
	$\Delta\lambda_{ST}$	5279	4718	6454	5558	5485	5204

View Article Online
DOI: 10.1039/C7NJ03142D

	Φ_{fl}	0.29	0.66	0.38	0.69	0.55	0.58
DMSO (45.1)	λ_{abs}	388	410	401	425	432	453
	λ_{em}	501	525	559	584	608	630
	$\Delta\lambda_{ST}$	5813	5342	7048	6406	6700	6202
	Φ_{fl}	0.57	0.80	0.73	0.76	0.76	0.72
MeCN (45.6)	λ_{abs}	371	400	380	413	414	440
	λ_{em}	479	515	527	566	566	610
	$\Delta\lambda_{ST}$	6077	5582	7340	6545	6486	6333
	Φ_{fl}	0.41	0.63	0.38	0.63	0.49	0.59
MeOH (54.4)	λ_{abs}	371	405	381	417	417	443
	λ_{em}	496	521	532	559	567	590
	$\Delta\lambda_{ST}$	6793	5497	7449	6091	6344	5624
	Φ_{fl}	0.30	0.61	0.25	0.64	0.47	0.43

See Table 2.

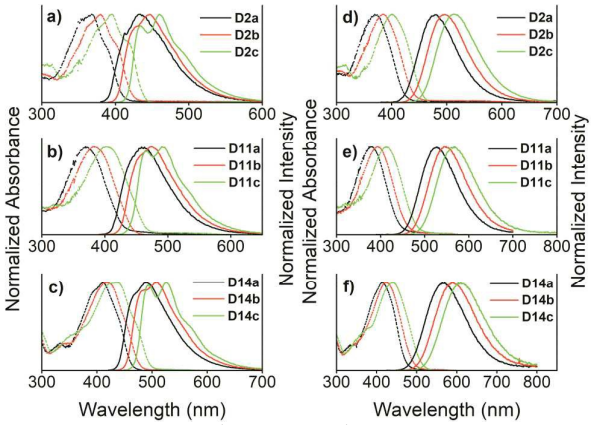

Figure 8. Absorption (dashed lines) and fluorescence emission (solid) spectra of dyes **D2a-c** (a and d), **D11a-c** (b and e) and **D14a-c** (c and f) in cyclohexane (left) and acetonitrile (right).

Conclusions

A series of 20 styryl-based solvatofluorochromic dyes was efficiently prepared from 6-amino-2-methylbenzothiazole. The dyes were synthesized in satisfactory overall yield, using a simple and practical synthetic route starting from commercially available and inexpensive materials. The ease of *N*-alkylation renders this position ideal as a prospective anchoring point for further (bio)conjugation. Spectroscopic studies coupled with DFT calculations have enabled the understanding of the relationship between structure and the photophysical properties of the presented dyes in terms of the electronic properties of the donor (first series **D1b-D9b**) and inductive effects associated with multiple 6-aminoalkylation. The dyes proved to be highly emissive in polar and nonpolar solvents. They are characterized by the formation of an intramolecular charge transfer excited states as corroborated by their large positive solvatochromic emission bands. High Stokes shifts, up to 192 and 255 nm, could be accessed for the phenyl and the polycyclic aromatic series, respectively. This highlights that the commonly used π-acceptors groups can be efficiently replaced by purely σ-acceptor to broadly tune the emission wavelength towards the red region. Finally, for dyes containing *para*-substituted phenyl rings, the perfect correlation between Hammett parameter (σ_P) and Stokes shifts and λ_{em} provides a complementary approach to anticipate photophysical properties of other members of this family of fluorescent probes. Using this correlation and the subtle changes brought by the 6-amino alkylation, specific fluorescent tools that absorb and emit in a particular spectral range can be easily designed. Our laboratories have expertise in the sensing of DNA/(bio)molecules interactions,[52-54] hence we envision to use of these finely-tunable dyes for this purpose.

Experimental Section

All solvents for absorption and fluorescence experiments were of spectroscopic grade. Absorption spectra were recorded on a Cary 4 spectrophotometer (Varian) using quartz cells of 1 cm path length. Fluorescence spectra were recorded on FluoroMax 4.0 spectrofluorometer (Jobin Yvon, Horiba). The wavelengths corresponding to the absorption maxima were used as the excitation wavelengths. Stock solutions of the solvatofluorochromic dyes were prepared using 1,4-dioxane. The samples used for spectroscopic measurements contained ≈ 0.1% v/v of the stock solvent. UV-vis absorption spectra were recorded using a dye concentration of *ca.* 10^{-5} M. Fluorescence emission spectra were recorded using a dye concentration of *ca.* 10^{-6} M. All chemical reagents were obtained from commercial sources (Aldrich, Acros, Alfa Aesar) and were used as supplied. The reactions were monitored by thin-layer chromatography (TLC, Merck silica gel 60 F254 plates) and visualized both by UV radiation (254 & 365 nm) and by spraying with a relevant staining agent followed by a subsequent warming with a heat gun. Column chromatography was performed with flash silica gel (40–63 mm). All NMR spectra (^{1}H, ^{13}C, ^{19}F) were recorded on Bruker Advance Spectrometers (200 or 400 MHz). ^{1}H NMR (200 and 400 MHz), ^{13}C{^{1}H} NMR (50 and 101 MHz), and ^{19}F{^{1}H} (188 and 377 MHz) spectra were obtained with samples dissolved in $CDCl_3$ or DMSO-d_6, with the solvent residual signals as internal references: 7.26 ppm for $CHCl_3$ and 2.50 ppm for DMSO-d_6 for ^{1}H NMR experiments, and 77.16 ppm for $CDCl_3$ and 39.52 ppm for DMSO-d_6 for ^{13}C NMR experiments.[55] Chemical shifts (δ) are given in ppm to the nearest 0.01 (^{1}H) or 0.1 ppm (^{13}C). The coupling constants (*J*) are given in Hertz (Hz). The signals are reported as follows: chemical shift, multiplicity (s = singlet, d =

View Article Online
DOI: 10.1039/C7NJ03142D

doublet, t = triplet, m = multiplet, dd = doublet of doublets, br = broad), coupling constants (*J*) and integration. Dye syntheses were performed in a Branson 5510 ultrasound bath. Low resolution mass spectra (MS) were recorded on an Esquire 3000 Plus apparatus with ESI in both positive and negative mode. High Resolution Mass Spectra (HRMS) were recorded on a ThermoFisher Q Exactive (ESIMS) at a resolution of 140000 at m/z 200. Density functional theory (DFT) and time-dependent DFT (TD-DFT) calculations were performed using the Gaussian03[56] software at the MPW1PW91/6-311+G(d,p) level of theory for all atoms without any symmetry restrictions. Optimized structures of the ground state were checked via a calculation of vibrational frequencies, ensuring that no imaginary frequencies were present. The vertical excitation energies are determined using the conventional TD-DFT procedure on the ground state geometries. The effects of solvents were taken into account by the polarizable continuum model (PCM). Supplementary data associated with this article include: photophysical characterizations, copies of NMR spectra - see Supporting Information for more details.

Benzothiazole precursors 2-5.

*2-methyl-6-nitrobenzo[d]thiazole (**2**).* In a 250 mL round-bottom flask were added 29.8 g (200 mmol) of 2-methylbenzothiazole and 100 mL of concentrated sulfuric acid. The mixture was cooled to 0°C and a solution of 17.0 g (200 mmol) of sodium nitrate in 100 mL of concentrated sulfuric acid was slowly added while keeping the temperature of the reaction media below 5 °C. After completion of the addition, the reaction was further stirred for 2 hours at 0°C before pouring the mixture into 1L of crushed ice. The precipitate formed was filtered off, and washed with cold water and ethanol. It was subsequently recrystallized from methanol to afford 28.7 g of light yellow solid. Yield: 74 %. ^{1}H NMR (200 MHz, $CDCl_3$) δ (ppm) 8.73 (d, *J* = 2.3 Hz, 1H), 8.29 (dd, *J* = 9.0, 2.3 Hz, 1H), 7.99 (d, *J* = 9.0 Hz, 1H), 2.89 (s, 3H). ^{13}C{^{1}H} NMR (50 MHz, $CDCl_3$) δ(ppm) 173.4, 157.2, 144.8, 136.1, 122.7, 121.6, 118.1, 20.8.

*6-amino-2-methylbenzo[d]thiazole (**3**).* To a solution of 19.4 g (100 mmol) of **2** in 200 mL of methanol, were successively added 6.5 g of zinc powder (100 mmol) and 25.4 g (400 mmol) of ammonium formate. The reaction was stirred overnight at room temperature. Then, the crude mixture was filtered over celite, the filtrate was diluted with ethyl acetate and extracted with water (3 × 200 mL). The organic phase was concentrated in *vacuo* and the crude residue was purified by flash chromatography on silica gel, using a 3/7 (v/v) mixture of cyclohexane/ethyl acetate as the eluent, to afford 12.6 g of compound **3** as a grey powder. Yield: 77 %. ^{1}H NMR (200 MHz, $CDCl_3$) δ (ppm) 7.68 (d, *J* = 8.6 Hz, 1H), 7.02 (d, *J* = 2.1 Hz, 1H), 6.76 (dd, *J* = 8.6, 2.3 Hz, 1H), 3.80 (br s, 2H), 2.73 (s, 3H). ^{13}C{^{1}H} NMR (50 MHz, $CDCl_3$) δ (ppm) 162.7, 146.8, 144.1, 137.3, 122.7, 115.2, 105.9, 19.9.

*N-(2-methylbenzo[d]thiazol-6-yl)acetamide (**4**).* In a 100 ml round-bottom flask, 4.9 g (30 mmol) of **3**, 6.1 g (60 mmol) of triethylamine and 0.3 g (3 mmol) of DMAP were dissolved in 30 mL of anhydrous DMF. The mixture was cooled to 0°C in an ice bath before the dropwise addition of acetyl chloride (2.35 mL, 33 mmol). After completion of the addition, the ice bath was removed and the mixture was stirred at r.t. for 1 hour. The solvent was removed under reduced pressure and the residue was dissolved in 100 mL of ethyl acetate, washed with water (3×100 mL) and brine (100 mL). The organic layer was dried over magnesium sulfate, filtered and the volatiles were removed in *vacuo*. Finally, the crude residue was purified by flash chromatography on silica gel, using cyclohexane/ethyl acetate (6/4, v/v) as the eluent, to afford 5,92 g of pure compound **4** as light yellow solid. Yield: 96 %. Mp: 139-140 °C. ^{1}H NMR (400 MHz, $CDCl_3$) δ (ppm) 8.39 (s, 1H), 8.08 (s, 1H), 7.82 (d, *J* = 8.7 Hz, 1H), 7.27 (d, *J* = 8.7 Hz, 1H), 2.81 (s, 3H), 2.21 (s, 3H). ^{13}C{^{1}H} NMR (50 MHz, $CDCl_3$) δ (ppm) 168.9, 166.6, 150.1, 136.6, 135.1, 122.3, 118.8, 112.6, 24.6, 20.1. HRMS (ESI) m/z: $[M + H]^+$ Calcd for $C_{10}H_{11}N_2OS$ 207.0587; Found 207.0588.

*6-ethylamino-2-methylbenzo[d]thiazole (**5**).* A 250 mL round-bottom flask was charged with 5.0 g (24 mmol) of **4**, and 100 mL of dry THF, under an inert atmosphere (Ar). To this mixture were slowly added 3.1 g (4 equiv.) of $LiAlH_4$ and the reaction was subsequently stirred overnight. The unreacted $LiAlH_4$ was quenched via the dropwise addition of acetone. The crude was neutralized with 1 M HCl and filtered over celite. The filtrate was concentrated to dryness, dissolved in 150 mL of ethyl acetate and washed with brine (3×150 mL). The organic layer was dried over magnesium sulfate, filtered and the volatiles were removed in *vacuo*. The crude was purified by flash chromatography on silica gel, using cyclohexane/ethyl acetate (8/2, v/v) as the eluent, to provide 4.0 g of precursor **5** as a grey solid. Yield: 87%. Mp: 107-108 °C. ^{1}H NMR (200 MHz, $CDCl_3$) δ (ppm) 7.68 (d, *J* = 8.7 Hz, 1H), 6.90 (d, *J* = 2.3 Hz, 1H), 6.69 (dd, *J* = 8.7, 2.4 Hz, 1H), 3.69 (br s, 1H), 3.15 (q, *J* = 7.1 Hz, 2H), 2.72 (s, 3H), 1.25 (t, *J* = 7.1 Hz, 3H). ^{13}C{^{1}H} NMR (50 MHz, $CDCl_3$) δ (ppm) 161.7, 146.3, 145.8, 137.7, 122.6, 113.9, 102.2, 38.8, 19.8, 14.8. HRMS (ESI) m/z: $[M + H]^+$ Calcd for $C_{10}H_{13}N_2S$ 193.0794; Found 193.0796.

General procedure for the synthesis of dyes D2a, D11a and D14a. 3 (1 equiv.) in DMF (0.2 M), potassium hydroxide (1 equiv.), and the aldehyde (1,3 equiv.) were subjected to ultrasonic irradiation for 1 hour at room temperature. The solvent was removed in *vacuo*, and the residue suspended in water. After acidification to pH 1 using concentrated HCl, the aqueous layer was extracted with ethyl acetate to remove the aldehyde in excess. The water layer was neutralized with NaOH (1M) and extracted with ethyl acetate. The organic layer was dried over magnesium sulfate, filtered and the volatiles were removed in *vacuo*. The crude was purified by flash column chromatography on silica gel using cyclohexane/ethyl acetate mixtures as the eluents. Finally, recrystallization from methanol afforded the desired dyes as bright solids.

Dye **D2a**.The crude product was purified using cyclohexane/ethyl acetate (8/2, v/v) as the eluent. Yield 59 %. Mp: 182-183 °C. ^{1}H NMR (400 MHz, $CDCl_3$) δ (ppm) 7.74 (d, *J* = 8.6 Hz, 1H), 7.49 (d, *J* = 8.7 Hz, 2H), 7.32 (d, *J* = 16.2 Hz, 1H), 7.22 (d, *J* = 16.2 Hz, 1H), 7.08 (d, *J* = 2.2 Hz, 1H), 6.92 (d, *J* = 8.7 Hz, 2H), 6.80 (dd, *J* = 8.6, 2.3 Hz, 1H), 3.84 (s, 5H). ^{13}C{^{1}H} NMR (101 MHz, $CDCl_3$) δ (ppm) 163.6, 160.6, 147.5, 144.7, 136.2, 135.8, 128.7, 128.6, 123.4, 120.5, 115.7, 114.5, 105.8, 55.5. HRMS (ESI) m/z: $[M + H]^+$ Calcd for $C_{16}H_{15}N_2OS$ 283.0899; Found 283.0900.

Dye **D11a**. The crude product was purified using cyclohexane/ethyl acetate (8/2, v/v) as the eluent. Yield 65 %. Mp: 194-195 °C. ^{1}H NMR (400 MHz, $CDCl_3$) δ (ppm) 8.25 (d, *J* = 8.4 Hz, 1H), 8.19 (d, *J* = 15.9 Hz, 1H), 7.88 (t, *J* = 8.8 Hz, 2H), 7.81 (t, *J* = 9.1 Hz, 2H), 7.61 - 7.50 (m, 3H), 7.44 (d, *J* = 16.0 Hz, 1H), 7.12 (s, 1H), 6.84 (d, *J* = 8.6 Hz, 1H), 3.88 (br s, 2H). ^{13}C{^{1}H} NMR (101 MHz, $CDCl_3$) δ (ppm) 163.1, 147.5, 145.0, 136.5, 133.9, 133.2, 132.9, 131.4, 129.5, 128.9, 126.7, 126.2, 125.8, 125.2, 124.4, 123.8, 123.6, 115.9, 105.8. HRMS (ESI) m/z: $[M + H]^+$ Calcd for $C_{19}H_{15}N_2S$ 303.0950; Found 303.0951.

Dye **D14a**.The crude product was purified using cyclohexane/ethyl acetate (7/3, v/v) as the eluent. Yield 46 %. Mp: 225 °C (decomp.). ^{1}H NMR (400 MHz, DMSO) δ (ppm) 8.66 (d, *J* = 9.4 Hz, 1H), 8.61 (d, *J* = 8.3 Hz, 1H), 8.48 (d, *J* = 15.9 Hz, 1H), 8.40 –

View Article Online
DOI: 10.1039/C7NJ03142D

8.31 (m, 4H), 8.23 (d, *J* = 1.7 Hz, 2H), 8.12 (t, *J* = 7.6 Hz, 1H), 7.81 (d, *J* = 15.9 Hz, 1H), 7.70 (d, *J* = 8.7 Hz, 1H), 7.12 (d, *J* = 2.1 Hz, 1H), 6.83 (dd, *J* = 8.7, 2.1 Hz, 1H), 5.58 (d, 2H). $^{13}C\{^1H\}$ NMR (101 MHz, DMSO) δ (ppm) 159.9, 147.7, 145.2, 136.2, 131.1, 130.9, 130.4, 130.3, 129.5, 128.2, 128.1, 127.8, 127.4, 126.5, 125.8, 125.5, 125.4, 124.9, 124.2, 123.9, 123.8, 123.1, 122.6, 115.1, 103.6. HRMS (ESI) m/z: $[M + H]^+$ Calcd for $C_{25}H_{17}N_2S$ 377.1107; Found 377.1113.

General procedure for the synthesis of dyes D1b-D14b. Precursor **5** (1 equiv.) in DMF (0.2 M), potassium hydroxide (1 equiv.) and aldehyde (1,3 equiv.) were subjected to ultrasonic irradiation for 1 hour at room temperature. The solvent was removed in *vacuo*, and the crude was purified by flash column chromatography on silica gel using cyclohexane/ethyl acetate mixtures as the eluents. Finally, recrystallization from methanol afforded the desired dyes as bright solids.

Dye **D1b**. The crude product was purified using cyclohexane/ethyl acetate (8/2, v/v) as the eluent. Yield 69 %. Mp: 119-120 °C. ^1H NMR (200 MHz, $CDCl_3$) δ (ppm) 7.75 (d, *J* = 8.8 Hz, 1H), 7.55 (dd, *J* = 8.0, 1.5 Hz, 2H), 7.45 – 7.30 (m, 5H), 6.95 (d, *J* = 2.3 Hz, 1H), 6.74 (dd, *J* = 8.8, 2.4 Hz, 1H), 3.68 (br s, 1H), 3.21 (q, *J* = 7.1 Hz, 2H), 1.30 (t, *J* = 7.1 Hz, 3H). $^{13}C\{^1H\}$ NMR (50 MHz, $CDCl_3$) δ (ppm) 162.2, 146.9, 146.4, 136.8, 135.9, 135.5, 129.0, 127.2, 123.5, 122.7, 114.7, 101.9, 38.8, 14.9. HRMS (ESI) m/z: $[M + H]^+$ Calcd for $C_{17}H_{17}N_2S$ 281.1107; Found 281.1108.

Dye **D2b**. The crude product was purified using cyclohexane/ethyl acetate (75/25, v/v) as the eluent. Yield 78 %. Mp: 134-135 °C. ^1H NMR (400 MHz, $CDCl_3$) δ (ppm) 7.73 (d, *J* = 8.8 Hz, 1H), 7.48 (d, *J* = 8.7 Hz, 2H), 7.30 (d, *J* = 16.2 Hz, 1H), 7.22 (d, *J* = 16.2 Hz, 1H), 6.94 (d, *J* = 2.3 Hz, 1H), 6.91 (d, *J* = 8.8 Hz, 2H), 6.73 (dd, *J* = 8.8, 2.3 Hz, 1H), 3.83 (s, 4H), 3.20 (q, *J* = 7.1 Hz, 2H), 1.29 (t, *J* = 7.1 Hz, 3H). $^{13}C\{^1H\}$ NMR (101 MHz, $CDCl_3$) δ (ppm) 162.6, 160.4, 146.8, 146.5, 136.6, 135.2, 128.7, 128.6, 123.3, 120.6, 114.5, 114.4, 102.0, 55.5, 38.8, 14.9. HRMS (ESI) m/z: $[M + H]^+$ Calcd for $C_{18}H_{19}N_2OS$ 311.1213; Found 311.1213.

Dye **D3b**. The crude product was purified using cyclohexane/ethyl acetate (8/2, v/v) as the eluent. Yield 48 %. Mp: 140-141 °C. ^1H NMR (200 MHz, $CDCl_3$) δ (ppm) 7.76 (d, *J* = 8.8 Hz, 1H), 7.63 (s, 4H), 7.44 (d, *J* = 16.3 Hz, 1H), 7.32 (d, *J* = 16.3 Hz, 1H), 6.96 (d, *J* = 2.3 Hz, 1H), 6.77 (dd, *J* = 8.8, 2.3 Hz, 1H), 3.85 (br s, 1H), 3.23 (q, *J* = 7.1 Hz, 2H), 1.31 (t, *J* = 7.1 Hz, 3H). $^{13}C\{^1H\}$ NMR (50 MHz, $CDCl_3$) δ (ppm) 161.2, 147.0, 146.5, 139.4, 137.1, 133.4, 130.4 (q, J = 32.6 Hz), 127.3, 125.9 (q, *J* = 3.8 Hz), 125.0, 123.8, 115.0, 101.9, 38.9, 14.8. $^{19}F\{^1H\}$ NMR (188 MHz, $CDCl_3$) δ (ppm) -62.6. HRMS (ESI) m/z: $[M + H]^+$ Calcd for $C_{18}H_{16}N_2F_3S$ 349.0981; Found 349.0983.

Dye **D4b**. The crude product was purified using cyclohexane/ethyl acetate (8/2, v/v) as the eluent. Yield 82 %. Mp: 178-179 °C. ^1H NMR (400 MHz, $CDCl_3$) δ (ppm) 7.75 (d, *J* = 8.8 Hz, 1H), 7.51 (d, *J* = 7.2 Hz, 2H), 7.40 (d, *J* = 7.2 Hz, 2H), 7.33 (d, *J* = 16.1 Hz, 1H), 7.26 (d, *J* = 16.2 Hz, 1H), 6.96 (s, 1H), 6.75 (d, *J* = 8.8 Hz, 1H), 3.96 (br s, 1H), 3.22 (q, *J* = 7.0 Hz, 2H), 1.31 (t, *J* = 7.0 Hz, 3H). $^{13}C\{^1H\}$ NMR (101 MHz, $CDCl_3$) δ (ppm) 161.7, 146.9, 146.5, 136.9, 134.9, 133.9, 132.2, 128.6, 123.6, 123.4, 122.9, 114.8, 101.9, 38.9, 14.9. HRMS (ESI) m/z: $[M + H]^+$ Calcd for $C_{17}H_{16}N_2BrS$ 359.0212; Found 359.0219.

Dye **D5b**. The crude product was purified using cyclohexane/ethyl acetate (8/2, v/v) as the eluent. Yield 74 %. Mp: 129-130 °C. ^1H NMR (400 MHz, $CDCl_3$) δ (ppm) 7.79 (d, *J* = 7.9 Hz, 1H), 7.77 (d, *J* = 8.8 Hz, 1H), 7.70 – 7.64 (m, 2H), 7.57 (t, *J* = 7.7 Hz, 1H), 7.41 (t, *J* = 7.7 Hz, 1H), 7.36 (d, *J* = 16.0 Hz, 1H), 6.96 (d, *J* = 2.3 Hz, 1H), 6.76 (dd, *J* = 8.8, 2.4 Hz, 1H), 3.99 (br s, 1H), 3.22 (q, *J* = 7.1 Hz, 2H), 1.31 (t, *J* = 7.1 Hz, 3H). $^{13}C\{^1H\}$ NMR (101 MHz, $CDCl_3$) δ (ppm) 161.5, 147.1, 146.6, 137.1, 134.9, 132.2, 130.8 (q, *J* = 1.9 Hz), 128.5, 128.1 (q, *J* = 30.0 Hz), 127.3, 126.7, 126.3 (q, *J* = 5.7 Hz), 124.4 (d, *J* = 273.9 Hz), 123.8, 114.9, 102.0, 38.9, 14.8. $^{19}F\{^1H\}$ NMR (188 MHz, $CDCl_3$) δ (ppm) -59.0. HRMS (ESI) m/z: $[M + H]^+$ Calcd for $C_{18}H_{16}N_2F_3S$ 349.0981; Found 349.0983.

Dye **D6b**. The crude product was purified using cyclohexane/ethyl acetate (75/25, v/v) as the eluent. Yield 79 %. 69-70 °C. ^1H NMR (200 MHz, $CDCl_3$) δ (ppm) 7.74 (d, *J* = 8.8 Hz, 1H), 7.64 (d, *J* = 16.5 Hz, 1H), 7.41 (d, *J* = 16.4 Hz, 1H), 7.23 (dd, *J* = 7.9, 1.3 Hz, 1H), 7.07 (t, *J* = 8.0 Hz, 1H), 6.94 (d, *J* = 2.2 Hz, 1H), 6.88 (dd, *J* = 8.1, 1.4 Hz, 1H), 6.73 (dd, *J* = 8.8, 2.3 Hz, 1H), 3.89 (s, 3H), 3.88 (s, 3H), 3.21 (q, *J* = 7.1 Hz, 2H), 1.29 (t, *J* = 7.1 Hz, 3H). $^{13}C\{^1H\}$ NMR (101 MHz, $CDCl_3$) δ (ppm) 162.8, 153.2, 147.6, 146.9, 146.4, 136.8, 130.2, 130.1, 124.4, 124.2, 123.5, 118.6, 114.5, 112.7, 101.9, 61.4, 55.9, 38.8, 14.8. HRMS (ESI) m/z: $[M + H]^+$ Calcd for $C_{19}H_{21}N_2O_2S$ 341.1318; Found 341.1321.

Dye **D7b**. The crude product was purified using cyclohexane/ethyl acetate (7/3, v/v) as the eluent. Yield 72 %. Mp: 50-51 °C. ^1H NMR (200 MHz, $CDCl_3$) δ (ppm) 7.65 (d, *J* = 8.8 Hz, 1H), 7.23 (d, *J* = 16.2 Hz, 1H), 7.14 (d, *J* = 16.3 Hz, 1H), 6.87 (d, *J* = 2.2 Hz, 1H), 6.70 – 6.63 (m, 3H), 3.82 (s, 6H), 3.80 (s, 3H), 3.13 (q, *J* = 7.1 Hz, 2H), 1.22 (t, *J* = 7.1 Hz, 3H). $^{13}C\{^1H\}$ NMR (50 MHz, $CDCl_3$) δ (ppm) 161.9, 153.5, 146.9, 146.3, 139.0, 136.7, 135.2, 131.6, 123.4, 122.2, 114.6, 104.2, 101.9, 61.1, 56.2, 38.8, 14.8. HRMS (ESI) m/z: $[M + H]^+$ Calcd for $C_{20}H_{23}N_2O_3S$ 371.1424; Found 371.1431.

Dye **D8b**. The crude product was purified using cyclohexane/ethyl acetate (85/15, v/v) as the eluent. Yield 36 %. Mp: 122-123 °C. ^1H NMR (400 MHz, $CDCl_3$) δ (ppm) 7.93 (s, 1H), 7.88 (d, *J* = 8.2 Hz, 1H), 7.83 – 7.73 (m, 2H), 7.62 (d, *J* = 16.1 Hz, 1H), 7.41 (d, *J* = 16.0 Hz, 1H), 6.93 (d, *J* = 1.9 Hz, 1H), 6.75 (dd, *J* = 8.8, 2.1 Hz, 1H), 3.89 (br s, 1H), 3.21 (q, *J* = 7.1 Hz, 2H), 1.30 (t, *J* = 7.1 Hz, 3H). $^{13}C\{^1H\}$ NMR (101 MHz, $CDCl_3$) δ (ppm) 160.4, 147.5, 146.4, 138.6, 137.4, 130.2 (q, *J* = 33.6 Hz), 129.0 (q, *J* = 3.4 Hz), 128.9, 128.7, 128.4 (q, *J* = 30.8 Hz), 127.8, 124.1, 123.5 (q, *J* = 274.3 Hz), 123.6 - 123.4 (m), 123.3 (q, *J* = 272.3 Hz), 115.1, 101.5, 38.7, 14.8. $^{19}F\{^1H\}$ NMR (377 MHz, $CDCl_3$) δ (ppm) -59.7, -62.9. HRMS (ESI) m/z: $[M + H]^+$ Calcd for $C_{19}H_{15}N_2F_6S$ 417.0855; Found 417.0856.

Dye **D9b**. The crude product was purified using cyclohexane/ethyl acetate (8/2, v/v) as the eluent. Yield 59 %. Mp: 148-149 °C. ^1H NMR (400 MHz, $CDCl_3$) δ (ppm) 7.72 (d, *J* = 8.7 Hz, 1H), 7.42 (d, *J* = 7.3 Hz, 2H), 7.14 (dd, *J* = 15.0, 10.4 Hz, 1H), 6.94 – 6.82 (m, 5H), 6.78 – 6.72 (m, 2H), 3.83 (s, 3H), 3.79 (br s, 1H), 3.22 (q, *J* = 6.7 Hz, 2H), 1.30 (t, *J* = 6.7 Hz, 3H). $^{13}C\{^1H\}$ NMR (101 MHz, $CDCl_3$) δ (ppm) 162.3, 160.0, 146.8, 146.6, 136.8, 136.4, 136.1, 129.7, 128.3, 125.9, 125.0, 123.3, 114.6, 114.4, 101.9, 55.5, 38.8, 14.9. HRMS (ESI) m/z: $[M + H]^+$ Calcd for $C_{20}H_{21}N_2OS$ 337.1369; Found 337.1370.

Dye **D10b**. The crude product was purified using cyclohexane/ethyl acetate (8/2, v/v) as the eluent. Yield 77 %. Mp: 194-195 °C. ^1H NMR (400 MHz, $CDCl_3$) δ (ppm) 7.76 (d, *J* = 8.8 Hz, 1H), 7.68 – 7.59 (m, 6H), 7.63 (s, 6H), 7.46 (t, *J* = 7.3 Hz, 2H), 7.42 – 7.33 (m, 3H), 6.97 (s, 1H), 6.75 (d, *J* = 8.8 Hz, 1H), 3.81 (br s, 1H), 3.23 (q, *J* = 6.9 Hz, 2H), 1.31 (t, *J* = 7.0 Hz, 3H). $^{13}C\{^1H\}$ NMR (101 MHz, $CDCl_3$) δ (ppm) 162.2, 147.0, 146.5, 141.7, 140.5, 136.9, 135.0, 134.9, 129.0, 127.7, 127.7, 127.6, 127.1, 123.5, 122.7, 114.7, 101.9, 38.8, 14.9. HRMS (ESI) m/z: $[M + H]^+$ Calcd for $C_{23}H_{21}N_2S$ 357.1420; Found 357.1421.

Dye **D11b**. The crude product was purified using cyclohexane/ethyl acetate (8/2, v/v) as the eluent. Yield 72 %. Mp: 116-117 °C. ^1H NMR (400 MHz, $CDCl_3$) δ (ppm) 8.26 (d, *J* = 8.1 Hz, 1H), 8.16 (d, *J* = 15.9 Hz, 1H), 7.84 (m, 4H), 7.55 (m, 3H), 7.44 (d, *J* = 15.8 Hz, 1H), 6.99 (s, 1H), 6.77 (d, *J* = 8.7 Hz, 1H), 3.89 (br s, 1H), 3.24 (q, *J* = 6.6 Hz, 1H), 1.32 (t, *J* = 6.9 Hz, 1H). $^{13}C\{^1H\}$ NMR (101

View Article Online
DOI: 10.1039/C7NJ03142D

MHz, $CDCl_3$) δ (ppm) 162.2, 147.0, 146.5, 136.9, 133.9, 133.4, 132.3, 131.3, 129.4, 128.9, 126.6, 126.2, 125.8, 125.3, 124.3, 123.7, 123.6, 114.7, 102.0, 38.9, 14.9. HRMS (ESI) m/z: $[M + H]^+$ Calcd for $C_{21}H_{19}N_2S$ 331.1263; Found 331.1264.

Dye **D12b**. The crude product was purified using cyclohexane/ethyl acetate (8/2, v/v) as the eluent. Yield 78 %. 74-75 °C. ^1H NMR (400 MHz, $CDCl_3$) δ (ppm) 8.27 (d, *J* = 8.6 Hz, 1H), 7.96 (d, *J* = 16.4 Hz, 1H), 7.84 - 7.76 (m, 3H), 7.69 (d, *J* = 16.4 Hz, 1H), 7.53 (t, *J* = 7.7 Hz, 1H), 7.39 (t, *J* = 7.4 Hz, 1H), 7.32 (d, *J* = 9.0 Hz, 1H), 6.99 (s, 1H), 6.76 (d, *J* = 8.7 Hz, 1H), 4.03 (s, 3H), 3.91 (br s, 1H), 3.23 (q, *J* = 7.1 Hz, 2H), 1.32 (t, *J* = 7.1 Hz, 3H). $^{13}C\{^1H\}$ NMR (101 MHz, $CDCl_3$) δ (ppm) 163.8, 156.0, 146.8, 146.6, 136.7, 132.6, 130.4, 129.3, 129.1, 128.7, 128.4, 127.2, 123.9, 123.7, 123.5, 118.2, 114.5, 113.0, 102.2, 56.4, 38.9, 14.9. HRMS (ESI) m/z: $[M + H]^+$ Calcd for $C_{22}H_{21}N_2OS$ 361.1369; Found 361.1369.

Dye **D13b**. The crude product was purified using cyclohexane/ethyl acetate (75/25, v/v) as the eluent. Yield 53 %. Mp: 180-181 °C. ^1H NMR (400 MHz, $CDCl_3$) δ (ppm) 8.45 (s, 1H), 8.42 – 8.34 (m, 2H), 8.27 (d, *J* = 16.4 Hz, 1H), 8.04 - 8.02 (m, 2H), 7.82 (d, *J* = 8.8 Hz, 1H), 7.53 – 7.48 (m, 4H), 7.29 (d, *J* = 16.4 Hz, 1H), 7.05 (d, *J* = 2.1 Hz, 1H), 6.81 (dd, *J* = 8.8, 2.2 Hz, 1H), 4.17 (br s, 1H), 3.27 (q, *J* = 7.1 Hz, 2H), 1.34 (t, *J* = 7.1 Hz, 3H). $^{13}C\{^1H\}$ NMR (101 MHz, $CDCl_3$) δ (ppm) 161.9, 146.8, 146.7, 136.9, 132.2, 131.6, 131.3, 130.8, 129.7, 128.9, 127.7, 126.2, 125.8, 125.5, 123.8, 114.9, 102.4, 39.1, 14.9. HRMS (ESI) m/z: $[M + H]^+$ Calcd for $C_{25}H_{21}N_2S$ 381.1420; Found 381.1422.

Dye **D14b**. The crude product was purified using cyclohexane/ethyl acetate (7/3, v/v) as the eluent. Yield 81 %. Mp: 179-180 °C. ^1H NMR (400 MHz, $CDCl_3$) δ (ppm) 8.51 (d, *J* = 9.3 Hz, 1H), 8.45 (d, *J* = 15.9 Hz, 1H), 8.34 (d, *J* = 8.1 Hz, 1H), 8.21 – 8.16 (m, 4H), 8.09 – 8.00 (m, 3H), 7.81 (d, *J* = 8.7 Hz, 1H), 7.62 (d, *J* = 15.9 Hz, 1H), 7.01 (d, *J* = 2.2 Hz, 1H), 6.79 (dd, *J* = 8.7, 2.3 Hz, 1H), 4.00 (br s, 1H), 3.25 (q, *J* = 7.1 Hz, 2H), 1.33 (t, *J* = 7.1 Hz, 3H).$^{13}C\{^1H\}$ NMR (101 MHz, $CDCl_3$) δ (ppm) 162.5, 146.9, 146.8, 137.0, 132.2, 131.9, 131.6, 131.0, 130.2, 129.0, 128.3, 128.1, 127.7, 126.3, 125.8, 125.6, 125.4, 125.2, 125.1, 125.0, 123.8, 123.6, 122.9, 114.8, 102.2, 38.9, 14.9. HRMS (ESI) m/z: $[M + H]^+$ Calcd for $C_{27}H_{21}N_2S$ 405.1420; Found 405.1420.

General procedure for the synthesis of dyes D2c, D11c and D14c. 6-ethylamino substituted dye **D2b**, **D11b** or **D14b** (1 equiv.) in acetonitrile (0.2 M), 1-iodooctane (3 equiv.) and potassium carbonate (3 equiv.) were heated to reflux during 24 hours in a sealed vial. The solvent was removed under reduced pressure and the crude was purified by flash column chromatography on silica gel, using cyclohexane/ethyl acetate mixtures as the eluents. Recrystallization from methanol afforded the desired dyes as bright solids.

Dye **D2c**. The crude product was purified using cyclohexane/ethyl acetate (95/5, v/v) as the eluent. Yield 86 %. Mp: 56-57 °C. ^1H NMR (400 MHz, $CDCl_3$) δ (ppm) 7.74 (d, *J* = 9.1 Hz, 1H), 7.47 (d, *J* = 8.7 Hz, 2H), 7.27 (d, *J* = 16.2 Hz, 1H), 7.20 (d, *J* = 16.2 Hz, 1H), 6.96 (d, *J* = 2.4 Hz, 1H), 6.90 (d, *J* = 8.7 Hz, 2H), 6.82 (dd, *J* = 9.1, 2.5 Hz, 1H), 3.82 (s, 3H), 3.41 (q, *J* = 7.0 Hz, 2H), 3.28 (t, *J* = 7.8 Hz, 2H), 1.64 – 1.58 (m, 2H), 1.33 – 1.24 (m, 10H), 1.18 (t, *J* = 7.0 Hz, 3H), 0.88 (t, *J* = 6.8 Hz, 3H). $^{13}C\{^1H\}$ NMR (101 MHz, $CDCl_3$) δ (ppm) 162.1, 160.4, 146.6, 145.1, 136.9, 134.9, 128.9, 128.6, 123.1, 120.8, 114.5, 112.7, 102.1, 55.5, 51.1, 45.6, 31.9, 29.6, 29.5, 27.7, 27.3, 22.8, 14.2, 12.5. HRMS (ESI) m/z: $[M + H]^+$ Calcd for $C_{26}H_{35}N_2OS$ 423.2465; Found 423.2465.

Dye **D11c**. The crude product was purified using cyclohexane/ethyl acetate (9/1, v/v) as the eluent. Yield 88 %. Mp: 44-45 °C. ^1H NMR (200 MHz, $CDCl_3$) δ (ppm) 7.75 (d, *J* = 8.8 Hz, 1H), 7.55 (dd, *J* = 8.0, 1.5 Hz, 2H), 7.45 – 7.30 (m, 5H), 6.95 (d, *J* = 2.3 Hz, 1H), 6.74 (dd, *J* = 8.8, 2.4 Hz, 1H), 3.68 (s, 1H), 3.21 (q, *J* = 7.1 Hz, 2H), 1.30 (t, *J* = 7.1 Hz, 3H). $^{13}C\{^1H\}$ NMR (50 MHz, $CDCl_3$) δ (ppm) 162.2, 146.9, 146.4, 136.8, 135.9, 135.5, 129.0, 127.2, 123.5, 122.7, 114.7, 101.9, 38.8, 14.9. HRMS (ESI) m/z: $[M + H]^+$ Calcd for $C_{29}H_{35}N_2S$ 443.2515; Found 443.2516.

Dye **D14c**. The crude product was purified using cyclohexane/ethyl acetate (9/1, v/v) as the eluent. Yield 80 %. Mp: 130-131 °C. ^1H NMR (400 MHz, $CDCl_3$) δ (ppm) 8.50 (d, *J* = 9.3 Hz, 1H), 8.41 (d, *J* = 15.9 Hz, 1H), 8.33 (d, *J* = 8.1 Hz, 1H), 8.20 - 8.14 (m, 4H), 8.08 – 7.99 (m, 3H), 7.85 (d, *J* = 9.0 Hz, 1H), 7.62 (d, *J* = 15.9 Hz, 1H), 7.04 (d, *J* = 1.9 Hz, 1H), 6.89 (dd, *J* = 9.0, 2.1 Hz, 1H), 3.45 (q, *J* = 6.9 Hz, 2H), 3.40 – 3.28 (t, *J* = 7.8 Hz), 1.73 - 1.59 (m, 2H), 1.37 – 1.32 (m, 10H), 1.23 (t, *J* = 7.0 Hz, 3H), 0.91 (t, *J* = 5.9 Hz, 3H). $^{13}C\{^1H\}$ NMR (101 MHz, $CDCl_3$) δ (ppm) 161.8, 146.9, 145.3, 137.3, 131., 131.7, 131.6, 131.0, 130.2, 128.9, 128.2, 127.9, 127.6, 126.3, 125.8, 125.5, 125.4, 125.2, 125.2, 125.0, 123.8, 123.5, 122.9, 112.9, 102.0, 51.1, 45.6, 31.9, 29.7, 29.5, 27.7, 27.4, 22.8, 14.2, 12.6. HRMS (ESI) m/z: $[M + H]^+$ Calcd for $C_{35}H_{37}N_2S$ 517.2672; Found 517.2674.

Conflicts of interest

There are no conflicts of interest to declare.

Acknowledgments

This work was supported by CNRS, University of Nice Sophia Antipolis and CAPES (fellowship to MSF, process number 99999.0011495/2015-01)

Associated Content

Supporting Information

Figures and tables, copies of ^1H, ^{19}F and ^{13}C NMR and HRMS spectra of all reported compounds, spectra from the photophysical study and additional data related to DFT calculation. This material is available free of charge via the Internet at http://pubs.acs.org.

References

1 A. S. Klymchenko, *Acc. Chem. Res.*, 2017, **50**, 366–375.

2 M. Dell'Acqua, L. Ronda, R. Piano, S. Pellegrino, F. Clerici, E. Rossi, A. Mozzarelli, M. L. Gelmi and G. Abbiati, *J. Org. Chem.*, 2015, **80**, 10939–10954.

3 Y. J. Lu, Z. Y. Wang, D. P. Hu, Q. Deng, B. H. Huang, Y. X. Fang, K. Zhang, W. L. Wong and C. F. Chow, *Dye. Pigment.*, 2015, **122**, 94–102.

4 M. Cheniour, D. Gueyrard, P. G. Goekjian, T. Granjon and O. Marcillat, *RSC Adv.*, 2016, **6**, 5547–5557.

View Article Online
DOI: 10.1039/C7NJ03142D

5 S. J. Lord, H. D. Lee, R. Samuel, R. Weber, N. Liu, N. R. Conley, M. A. Thompson, R. J. Twieg and W. E. Moerner, *J. Phys. Chem. B*, 2010, **114**, 14157–14167.
6 A. Herner, I. Nikić, M. Kállay, E. A. Lemke and P. Kele, *Org. Biomol. Chem.*, 2013, **11**, 3297–3306.
7 Á. Eördögh, J. Steinmeyer, K. Peewasan, U. Schepers, H. A. Wagenknecht and P. Kele, *Bioconjug. Chem.*, 2016, **27**, 457–464.
8 C. Kuo and R. M. Hochstrasser, *J. Am. Chem. Soc.*, 2011, **133**, 4664–4667.
9 Y. Niko, P. Didier, Y. Mely, G. Konishi and A. S. Klymchenko, *Sci. Rep.*, 2016, **6**, 18870.
10 Y. Ni, R. K. Kannadorai, S. W.-K. Yu, Y.-T. Chang and J. Wu, *Org. Biomol. Chem.*, 2017, **15**, 4531–4535.
11 L. Zhu, A. H. Younes, Z. Yuan and R. J. Clark, *J. Photochem. Photobiol. A Chem.*, 2016, **311**, 1–15.
12 S. Achelle, J. Rodríguez-López, F. Bureš and F. Robin-Le Guen, *Dye. Pigment.*, 2015, **121**, 305–311.
13 H. Imahori, T. Umeyama and S. Ito, *Acc. Chem. Res.*, 2009, **42**, 1809–1818.
14 Y. Lin, Y. Li and X. Zhan, *Chem. Soc. Rev.*, 2012, **41**, 4245–4272.
15 A. Szlapa, S. Kula, U. Blaszkiewicz, M. Grucela, E. Schab-Balcerzak and M. Filapek, *Dye. Pigment.*, 2016, **129**, 80–89.
16 Y. Zhu and X. Wang, *Dye. Pigment.*, 2013, **97**, 222–229.
17 R. Wei, Z. Xu, X. Liu, Y. He and X. Wang, *J. Mater. Chem. C*, 2015, **3**, 10925–10933.
18 P. Xiao, M. Frigoli, F. Dumur, B. Graff, D. Gigmes, J. P. Fouassier and J. Laleve, *Macromolecules*, 2014, **47**, 106–112.
19 M. Pawlicki, H. A. Collins, R. G. Denning and H. L. Anderson, *Angew. Chemie - Int. Ed.*, 2009, **48**, 3244–3266.
20 C. Reichardt, *Chem. Rev.*, 1994, **94**, 2319–2358.
21 A. Marini, A. Munnoz-Losa, A. Biancardi and B. Mennucci, *J. Phys. Chem. B*, 2010, **114**, 17128–17135.
22 T. Deligeorgiev, A. Vasilev, S. Kaloyanova and J. J. Vaquero, *Color. Technol.*, 2010, **126**, 55–80.
23 E. Yalçin, S. Achelle, Y. Bayrak, N. Sefero□lu, A. Barsella and Z. Sefero□lu, *Tetrahedron Lett.*, 2015, **56**, 2586–2589.
24 R. P. Tayade and N. Sekar, *Dye. Pigment.*, 2016, **128**, 111–123.
25 P. G. Umape, Y. Gawale and N. Sekar, *J. Fluoresc.*, 2014, **24**, 1087–1098.
26 U. N. Yadav, H. S. Kumbhar, S. S. Deshpande, S. K. Sahoo and G. S. Shankarling, *RSC Adv.*, 2015, **5**, 42971–42977.
27 B. Jędrzejewska, B. Ośmiałowski and R. Zaleśny, *Photochem. Photobiol. Sci.*, 2016, **15**, 117–128.
28 R. D. Telore and N. Sekar, *Dye. Pigment.*, 2016, **129**, 1–8.
29 A. Szukalski, K. Parafiniuk, K. Haupa, W. Goldeman, B. Sahraoui, F. Kajzar and J. Mysliwiec, *Dye. Pigment.*, 2017, **142**, 507–515.
30 B. Vidya, M. Iniya, G. Sivaraman, R. V. Sumesh and D. chellappa, *Sensors Actuators, B Chem.*, 2017, **242**, 434–442.
31 K. Matsumura, M. Ono, A. Kitada, H. Watanabe, M. Yoshimura, S. Iikuni, H. Kimura, Y. Okamoto, M. Ihara and H. Saji, *J. Med. Chem.*, 2015, **58**, 7241–7257.
32 M. Ono, S. Hayashi, H. Kimura, H. Kawashima, M. Nakayama and H. Saji, *Bioorganic Med. Chem.*, 2009, **17**, 7002–7007.
33 N. V. Bashmakova, Y. O. Shaydyuk, S. M. Levchenko, A. E. Masunov, O. V. Przhonska, J. L. Bricks, O. D. Kachkovsky, Y. L. Slominsky, Y. P. Piryatinski, K. D. Belfield and M. V. Bondar, *J. Phys. Chem. A*, 2014, **118**, 4502–4509.
34 V. Hrobáriková, P. Hrobárik, P. Gajdoš, I. Fitilis, M. Fakis, P. Persephonis and P. Zahradník, *J. Org. Chem.*, 2010, **75**, 3053–3068.
35 T. Peng and D. Yang, *Org. Lett.*, 2010, **12**, 496–499.
36 B. Strehmel, A. M. Sarker and H. Detert, *ChemPhysChem*, 2003, **4**, 249–259.
37 A. R. Morales, A. Frazer, A. W. Woodward, H. Y. Ahn-White, A. Fonari, P. Tongwa, T. Timofeeva and K. D. Belfield, *J. Org. Chem.*, 2013, **78**, 1014–1025.
38 J. Shaya, F. Fontaine-Vive, B. Y. Michel and A. Burger, *Chem. - A Eur. J.*, 2016, **22**, 10627–10637.
39 A. Herner, I. Nikić, M. Kállay, E. A. Lemke and P. Kele, *Org. Biomol. Chem.*, 2013, **11**, 3297.
40 C. Würth, M. Grabolle, J. Pauli, M. Spieles and U. Resch-genger, *Nat. Protoc.*, 2013, **8**, 1535–50.
41 K. Kundu, S. F. Knight, N. Willett, S. Lee, W. R. Taylor and N. Murthy, *Angew. Chemie - Int. Ed.*, 2009, **48**, 299–303.
42 A. V. Kulinich, A. A. Ishchenko, A. K. Chibisov and G. V. Zakharova, *J. Photochem. Photobiol. A Chem.*, 2014, **274**, 91–97.
43 A. V Kulinich and A. A. Ishchenko, *Russ. Chem. Rev.*, 2009, **78**, 141–164.
44 V. A. Galievsky, S. I. Druzhinin, A. Demeter, P. Mayer, S. A. Kovalenko, T. A. Senyushkina and K. A. Zachariasse, *J. Phys. Chem. A*, 2010, **114**, 12622–12638.
45 X. Liu, J. M. Cole and Z. Xu, *J. Phys. Chem. C*, 2017, **121**, 13274–13279.
46 K. Rurack, M. L. Dekhtyar, J. L. Bricks, U. Resch-Genger and W. Rettig, *J. Phys. Chem. A*, 1999, **103**, 9626–9635.
47 E. Lippert, *Zeitschrift fur Naturforsch. - Sect. A J. Phys. Sci.*, 1955, **10**, 541–545.
48 N. Mataga, Y. Kaifu and M. Koizumi, *Bull. Chem. Soc. Jpn.*, 1956, **29**, 465–470.
49 C. Hansch, a Leo and R. W. Taft, *Chem. Rev.*, 1991, **91**, 165–195.
50 M. M. Martin, P. Plaza and P. Changenet-barret, *J. Phys. Chem. A*, 2002, **106**, 2351–2358.
51 T. Okada, T. Fujita, M. Kubota, S. Masaki, R. Ide, Y. Sakata and S. Mlsuiw, *Chem. Phys. Lett.*, 1972, **14**, 563–568.
52 D. Dziuba, V. Y. Postupalenko, M. Spadafora, A. S. Klymchenko, V. Guerineau, Y. Mely, R. Benhida and A. Burger, *J. Am. Chem. Soc.*, 2012, **134**, 10209–10213
53 J.-P. Joly, G. Mata, P. Eldin, L. Briant, F. Fontaine-Vive, M. Duca and R. Benhida, *Chem. Eur. J.*, 2014, **20**, 2071–

View Article Online
DOI: 10.1039/C7NJ03142D

2079.

54 M. Safir Filho, A. R. Martin and R. Benhida, *Bioorg. Med. Chem. Lett.*, 2017, **27**, 1780–1783

55 G. R. Fulmer, A. J. M. Miller, N. H. Sherden, H. E. Gottlieb, A. Nudelman, B. M. Stoltz, J. E. Bercaw and K. I. Goldberg, *Organometallics*, 2010, **29**, 2176–2179.

56 Gaussian 03, Revision C.02, M. J. Frisch, G. W. Trucks, H. B. Schlegel, G. E. Scuseria, M. A. Robb, J. R. Cheeseman, J. A. Montgomery, Jr., T. Vreven, K. N. Kudin, J. C. Burant, J. M. Millam, S. S. Iyengar, J. Tomasi, V. Barone, B. Mennucci, M. Cossi, G. Scalmani, N. Rega, G. A. Petersson, H. Nakatsuji, M. Hada, M. Ehara, K. Toyota, R. Fukuda, J. Hasegawa, M. Ishida, T. Nakajima, Y. Honda, O. Kitao, H. Nakai, M. Klene, X. Li, J. E. Knox, H. P. Hratchian, J. B. Cross, V. Bakken, C. Adamo, J. Jaramillo, R. Gomperts, R. E. Stratmann, O. Yazyev, A. J. Austin, R. Cammi, C. Pomelli, J. W. Ochterski, P. Y. Ayala, K. Morokuma, G. A. Voth, P. Salvador, J. J. Dannenberg, V. G. Zakrzewski, S. Dapprich, A. D. Daniels, M. C. Strain, O. Farkas, D. K. Malick, A. D. Rabuck, K. Raghavachari, J. B. Foresman, J. V. Ortiz, Q. Cui, A. G. Baboul, S. Clifford, J. Cioslowski, B. B. Stefanov, G. Liu, A. Liashenko, P. Piskorz, I. Komaromi, R. L. Martin, D. J. Fox, T. Keith, M. A. Al-Laham, C. Y. Peng, A. Nanayakkara, M. Challacombe, P. M. W. Gill, B. Johnson, W. Chen, M. W. Wong, C. Gonzalez, and J. A. Pople, Gaussian, Inc., Wallingford CT, 2004.